MNDO–Effective Charge Model Study of Solvent Effect on the Potential Energy Surface of the S_N2 Reaction

Teruya Kozaki, Kenji Morihashi, and Osamu Kikuchi*

Contribution from the Department of Chemistry, The University of Tsukuba, Tsukuba 305, Japan. *Received May 2, 1988*

Abstract: The potential energy surfaces of the S_N2 reactions $Cl^- + CH_3Cl$ and $F^- + CH_3Cl$ in solution were examined by MNDO–effective charge model calculations in which the solvent effect was introduced into the MNDO Fock matrix elements through the dielectric constant, ϵ, of the solvent. From the potential energy diagrams calculated for $\epsilon = 1.0$, 2.0, and 5.0, it was shown that the potential energy curve changes shape from the double-well type to the unimodal type when ϵ increases. This agrees well with experiment, and the MNDO–effective charge model is shown to reproduce correctly the differential solvation of each stage on the reaction coordinate.

The S_N2 reaction of an anion with a dipole molecule

$$X^- + CH_3Y \rightarrow XCH_3 + Y^-$$

has been extensively investigated in the gas phase as well as in solution.[1] The reaction in solution is much slower than that in the gas phase. To elucidate the cause of this remarkable difference, many experimental and theoretical efforts have been made.[2-8] Brauman et al.[2] compared the absolute rate of the S_N2 reactions in the gas phase and in solution and concluded that the potential energy surface of the S_N2 reaction in the gas phase is a double-well type, while it is a unimodal one in solution.

Bohme et al.[3,4] studied the S_N2 reaction in hydrated gas clusters by the flowing afterglow technique and found that the reaction rate decreases with stepwise hydration. In response to their experiments, Morokuma and Ohta[5] calculated the potential energy surface of the reactions $Cl^- + CH_3Cl$ and $OH^- + CH_3Cl$ by using ab initio MO methods. It was shown that the activation energy varies with the hydration number and the position to which the water molecules are attached and that the increase of the hydration number at the nucleophilic anion makes the activation energy large. Besides these works, there are some supermolecule calculations involving solvent[6] and many ab initio calculations without solvent[7] for S_N2 reactions.

Chandrasekhar et al.[8] examined the potential energy surface of the S_N2 reaction in solution by means of Monte Carlo simulation, in conjunction with ab initio 6-31G* calculations. A unimodal type potential was obtained by Monte Carlo simulation, while a double-well type potential was obtained by ab initio calculations without solvent.

Theoretical efforts to include solvent effects into quantum chemical calculations have been given extensively.[5,6,8-22] An approach using the effective charge model is one of them.[9-12] In the effective charge model, the solvation energy is estimated from the electrostatic interaction between the solute molecule, which consists of charged atoms, and the solvent, which is a dielectric medium with a dielectric constant of ϵ. This model has been correctly introduced into the CNDO Fock matrix elements by Tapia[10] and Constanciel and Contreras.[13] Using their scheme, we developed the MNDO–effective charge model method[14] based on the MNDO MO method.[23] Since this method is a semiempirical one, the molecular and electronic structures in solution can easily be estimated as a function of the dielectric constant of the solvent.

This paper considers the solvent effect on the potential energy profiles of S_N2 reactions on the basis of the MNDO–effective charge model calculations. The potential energy diagrams and maps were calculated as a function of the dielectric constant of the solvent. We show that this method correctly reproduces the effect of differential solvation on the potential energy surface and that the shift of the potential energy profile from the double-well type in the gas phase to the unimodal type in solution is caused by this differential solvation. Changes in the molecular structures and in the charge distribution of the system were also examined.

Method of Calculation

The effective charge model describes a solute molecule as an assembly of fractional charges on the nuclei that interact with the solvent. The solvation energy of the molecule has been given by Hoijting et al.[11] and Chalvet and Jano[12] as the generalized Born formula

(1) Parker, A. J. *Chem. Rev.* **1969**, *69*, 1.
(2) (a) Olmstead, W. N.; Brauman, J. I. *J. Am. Chem. Soc.* **1977**, *99*, 4219. (b) Pellerite, M. J.; Brauman, J. I. *Ibid.* **1980**, *102*, 5993.
(3) Tanaka, K.; Mackay, G. I.; Payzant, J. D.; Bohme, D. K. *Can. J. Chem.* **1976**, *54*, 1643.
(4) (a) Bohme, D. K.; Mackay, G. I.; Payzant, J. D. *J. Am. Chem. Soc.* **1974**, *96*, 4027. (b) Mackay, G. I.; Bohme, D. K. *Ibid.* **1978**, *100*, 327. (c) Bohme, D. K.; Mackay, G. I.; Tanner, S. D. *Ibid.* **1979**, *101*, 3724. (d) Bohme, D. K.; Mackay, G. I. *Ibid.* **1981**, *103*, 978. (e) Bohme, D. K.; Raksit, A. B. *Ibid.* **1984**, *106*, 3447.
(5) (a) Morokuma, K. *J. Am. Chem. Soc.* **1982**, *104*, 3732. (b) Ohta, K.; Morokuma, K. *J. Phys. Chem.* **1985**, *89*, 5845.
(6) (a) Cremaschi, P.; Gamba, A.; Simonetta, M. *Theor. Chim. Acta* **1972**, *25*, 237. (b) Jaume, J.; Lluch, J. M.; Oliva, A.; Bertran, J. *Chem. Phys. Lett.* **1984**, *106*, 232.
(7) (a) Dedieu, A.; Veillard, A. *J. Am. Chem. Soc.* **1972**, *94*, 6730. (b) Bader, R. F. W.; Duke, A. J.; Messer, R. R. *Ibid.* **1973**, *95*, 7715. (c) Keil, F.; Ahlrichs, R. *Ibid.* **1976**, *98*, 4787. (d) Fujimoto, H.; Inagaki, S. *Ibid.* **1977**, *99*, 7424. (e) Talaty, E. R.; Woods, J. J.; Simons, G. *Aust. J. Chem.* **1979**, *32*, 2289. (f) Wolfe, S.; Mitchell, D. J. *J. Am. Chem. Soc.* **1981**, *103*, 7692. (g) Carrion, F.; Dewar, M. J. S. *Ibid.* **1984**, *106*, 3531.
(8) (a) Chandrasekhar, J.; Smith, S. F.; Jorgensen, W. L. *J. Am. Chem. Soc.* **1984**, *106*, 3049. (b) Chandrasekhar, J.; Smith, S. F.; Jorgensen, W. L. *Ibid.* **1985**, *107*, 154. (c) Chandrasekhar, J.; Jorgensen, W. L. *Ibid.* **1985**, *107*, 2974.
(9) Tapia, O. *Molecular Interactions*; Ratajczak, H., Orville-Thomas, W. J., Eds.; Wiley: New York, 1982; Vol. 3, p 47.
(10) Tapia, O. *Quantum Theory of Chemical Reactions*; Daudel, A., Pullman, A., Salem, L., Veillard, A., Eds.; Reidel: Dordrecht, 1981; Vol. II, p 25.
(11) Hoijting, G. J.; de Boer, E.; van der Meij, P. H.; Weijland, W. P. *Recl. Trav. Chim. Pays-Bas* **1956**, *75*, 487.
(12) (a) Chalvet, O.; Jano, I. *C. R. Seances Acad. Sci.* **1964**, *259*, 1867. (b) Jano, I. *Ibid.* **1965**, *261*, 103.
(13) Constanciel, R.; Contreras, R. *Theor. Chim. Acta* **1984**, *65*, 1.
(14) Kozaki, T.; Morihashi, K.; Kikuchi, O. *J. Mol. Struct.* **1988**, *168*, 265.
(15) Klopman, G. *Chem. Phys. Lett.* **1967**, *1*, 200.
(16) Sinanoglue, O. *Theor. Chim. Acta* **1974**, *33*, 279.
(17) Germer, H. A., Jr. *Theor. Chim. Acta* **1974**, *34*, 145; **1974**, *35*, 273.
(18) Tapia, O. *Theor. Chim. Acta* **1978**, *47*, 157.
(19) Constanciel, R.; Tapia, O. *Theor. Chim. Acta* **1978**, *48*, 75.
(20) Constanciel, R.; Contreras, R. *C. R. Seances Acad. Sci.* **1983**, *296*, 333; **1983**, *296*, 417.
(21) Contreras, R.; Aizman, A. *Int. J. Quant. Chem.* **1985**, *27*, 293.
(22) Burshtein, K. Ya. *J. Mol. Struct.* **1987**, *153*, 195, 203, 209.
(23) (a) Dewar, M. J. S.; Thiel, W. *J. Am. Chem. Soc.* **1977**, *99*, 4899, 4907. (b) Dewar, M. J. S.; Rzepa, H. S. *Ibid.* **1978**, *100*, 784.

0002-7863/89/1511-1547$01.50/0

$$E^{solv} = -\frac{1}{2}(1 - \epsilon^{-1})\sum_A \frac{Q_A^2}{r_A} - \frac{1}{2}(1 - \epsilon^{-1})\sum_A \sum_{B \neq A} \frac{Q_A Q_B}{R_{AB}} \quad (1)$$

where ϵ is the dielectric constant of the solvent, A and B are atoms in the molecule, Q_A is the fractional charge of atom A, r_A is the radius of the charged atom A, and R_{AB} is the distance between A and B. The energy of the molecule in solution is the sum of the energy of the molecule in its isolated state and the solvation energy. The correct variational results, including the above solvation energy, have been given by Tapia[10] and Constanciel and Contreras.[13] Using their scheme, we have incorporated the effective charge model into the MNDO method.[14] The Fock matrix elements derived are

$$F_{rr} = F_{rr}^0 + (1 - \epsilon^{-1})\sum_B Q_B \Gamma_{AB} \quad (r \in A)$$

$$F_{rs} = F_{rs}^0 \quad (r \neq s) \quad (2)$$

where F_{rr}^0 and F_{rs}^0 are the Fock elements for an isolated molecule, and Γ_{AB} are evaluated by

$$\Gamma_{AA} = 1/r_A$$

$$\Gamma_{AB} = 1/\sqrt{R_{AB}^2 + \alpha^2}, \qquad \alpha = \tfrac{1}{2}(r_A + r_B) \quad (3)$$

It is necessary to evaluate atomic radii to calculate the Fock matrix elements. We adopted a set of radii based on the van der Waals radii.[26,27] The values used in this paper are 1.2, 1.7, 1.35, and 1.8 Å for H, C, F, and Cl, respectively.

In previous papers,[14,26b] we introduced the structural factor that estimates the degree to which the interaction between a charged atom and the solvent is weakened if the atom is located inside the molecule. This factor is important in the conformational analysis of a large molecule in solution. However, this factor was not used in the present work so that the intrinsic character of the solute–solvent interactions given in eq 1 would be reflected in the complicated potential energy surfaces.

The following S_N2 reactions were studied in this paper:

$$Cl^- + CH_3Cl \rightarrow ClCH_3 + Cl^- \quad (A)$$

$$F^- + CH_3Cl \rightarrow FCH_3 + Cl^- \quad (B)$$

Reaction A is an isoenergetic reaction, while reaction B is an exothermic one. The S_N2 reaction was assumed to be initiated by the backside attack of the ion on methyl chloride, and C_{3v} symmetry was assumed for the reaction system; i.e., the nucleophilic anion and the leaving Cl^- were set on the C_{3v} axis.

The geometry was optimized at five characteristic points on the potential energy surface: (i) the separated reactants, denoted by S_R; (ii) the association complex on the reactant side, C_R; (iii) the transition state, T; (iv) the association complex on the product side, C_P; and (v) the separated product, S_P. In order to locate the transition state, the norm of the gradient of the potential energy function was minimized[27] by assuming D_{3h} symmetry for reaction A and C_{3v} symmetry for reaction B. In order to represent the potential energy diagram, the reaction coordinate, r_c, used by Chandrasekhar et al.,[8] was adopted:

$$r_c = r_l - r_n \quad (4)$$

where r_l and r_n are the distances from the carbon atom to the leaving group and to the nucleophile, respectively.

The potential energy curve along the reaction coordinate, r_c, was obtained from the geometry-optimized energies for 40 points between $r_c = -6$ Å and $r_c = 6$ Å by spline interpolation. The changes in the atomic charges and geometrical parameters were also obtained along this reaction coordinate. The two-dimensional potential energy map was drawn for the two variables, r_n and r_l. For each point on the map, (r_n, r_l), the geometry was optimized and the energy was obtained. The energy was calculated for each 0.1–0.2 Å on the map, and the isoenergetic curves were obtained by interpolation.

Table I. Bond Lengths (Å) and Bond Angles (Deg) of the S_R, C_R, and T States of Reaction A

state	bond lengths and angles	ϵ = 1.0	ϵ = 2.0	ϵ = 5.0	ϵ = 80
S_R	C–Cl	1.795	1.813	1.834	1.847
	C–H	1.102	1.101	1.098	1.098
	Cl–C–H	108.1	107.2	106.2	105.7
C_R	C–Cl	1.830	1.833	1.847	1.854
	C–Cl′	3.345	3.798	3.801	3.800
	C–H	1.100	1.099	1.097	1.098
	Cl–C–H	106.5	106.4	105.8	105.5
T	C–Cl	2.149	2.209	2.288	2.386
	C–Cl′	2.149	2.209	2.288	2.386
	C–H	1.093	1.090	1.087	1.086
	Cl–C–H	90.0	90.0	90.0	90.0

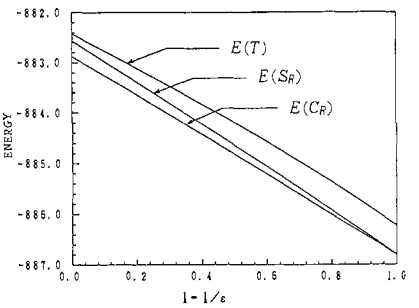

Figure 1. ϵ-Dependence of molecular energies (eV) for the separated reactants $E(S_R)$, the association complex $E(C_R)$, and the transition state $E(T)$ in the $Cl^- + CH_3Cl$ reaction.

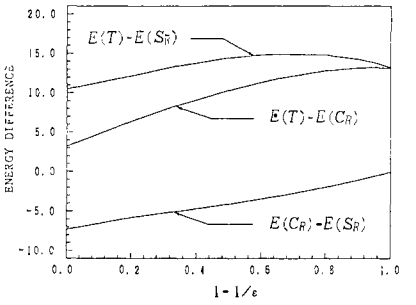

Figure 2. ϵ-Dependence of energy differences (kcal/mol) between states in the $Cl^- + CH_3Cl$ reaction.

Results and Discussion

Reaction of Methyl Chloride with Chloride Ion. Reaction A is an isoenergetic reaction and the potential energy surface must be symmetrical. Thus the behavior of the nucleophilic Cl^- ion can be understood from that of the leaving Cl^- ion by going back along the reaction coordinate. We will describe the results for only the leaving Cl^- ion.

The molecular structures of the S_R, C_R, and T states were optimized for ϵ = 1.0, 2.0, 5.0, and 80 and are shown in Table I. The distance between the carbon atom and the Cl anion of the association complex is largely affected by the dielectric constant of the solvent. The ϵ-dependence of molecular energies for the S_R, C_R, and T states is shown in Figure 1. All states are stabilized when ϵ increases. When $\epsilon \rightarrow \infty$, $E(C_R)$ happens to be equal to $E(S_R)$; i.e., the potential well corresponding to the complex vanishes. The ϵ-dependence of the energy differences between the states is shown in Figure 2. The energy difference $E(C_R) - E(S_R)$, which represents the depth of the potential well of the complex, becomes small with an increase of ϵ. The energy differences $E(T) - E(C_R)$ and $E(T) - E(S_R)$ are the intrinsic and the apparent energy barriers, respectively. The former increases monotonously with respect to ϵ, while the latter has a maximum in the curve. These trends indicate that the activation energy

(24) Born, M. *Z. Phys.* **1920**, *1*, 45.
(25) (a) Ohno, K. *Theor. Chim. Acta* **1964**, *2*, 219. (b) Klopman, G. *J. Am. Chem. Soc.* **1964**, *86*, 4550.
(26) Pauling, L. *The Nature of the Chemical Bond*, 3rd ed.; Cornell University Press: Ithaca, NY, 1960. (b) Kikuchi, O.; Kozaki, T.; Morihashi, K. *Nippon Kagaku Kaishi* **1986**, *11*, 1409.
(27) McIver, J. W., Jr.; Komornicki, A. *J. Am. Chem. Soc.* **1972**, *94*, 2625.

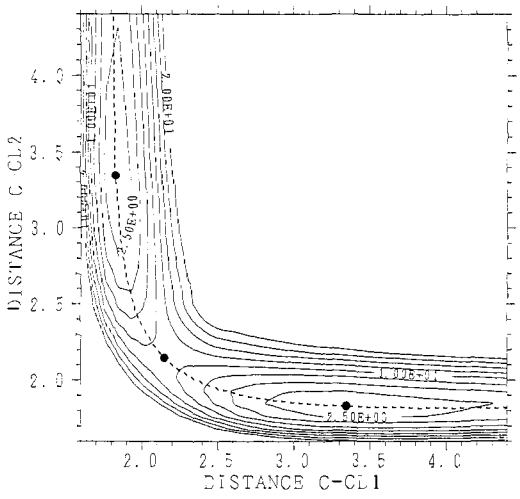

Figure 3. Potential energy map of the $CH_3Cl + Cl^-$ reaction for $\epsilon = 1.0$. The contours are drawn in steps of 2.5 kcal/mol. The values are relative to that for the association complex, which is the lowest energy point in the map. The dashed line indicates the reaction path along the reaction coordinate, r_c. The dots indicate the association complexes and the transition state. The C–Cl distances are in angstroms.

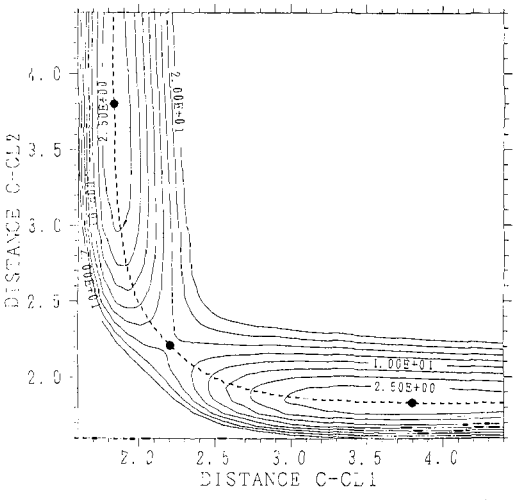

Figure 4. Potential energy map of the $CH_3Cl + Cl^-$ reaction for $\epsilon = 2.0$. See caption of Figure 3.

barrier is larger in solution ($\epsilon > 1$) than in the gas phase ($\epsilon = 1$). Figure 2 shows that the energy differences $E(T) - E(C_R)$ and $E(T) - E(S_R)$ are almost constant for $\epsilon > 5$, and the ϵ-dependence of the potential energy curve may be well understood from the results calculated for $\epsilon = 1$, 2, and 5.

Two-dimensional potential energy maps for $\epsilon = 1.0$, 2.0, and 5.0 are shown in Figure 3–5. The contour lines are drawn in steps of 2.5 kcal/mol. The broken lines are approximations for the minimum-energy reaction paths (MERP), and the closed circles on the curves indicate the association complexes and the transition state. The potential energy surface becomes flatter overall when ϵ increases, yet the activation energy of the reaction increases.

The energy profile along the MERP is shown in Figure 6 as a function of the reaction coordinate, r_c. The transition state on the reaction coordinate is located at $r_c = 0$. The association complex moves away from the transition state with increasing ϵ; this may be seen in Figure 6 and also in the calculated C–Cl distance of the association complex (see Table I). The depth of the potential energy well, $E(C_R) - E(S_R)$, the apparent energy barrier, $E(T) - E(S_R)$, and the intrinsic barrier, $E(T) - E(C_R)$, are given in Table II. As may be seen from Table II, the MNDO method ($\epsilon = 1.0$) gives values that are consistent with experiment in the gas phase[8,28] and with ab initio 6-31G* calculations[8] in the gas phase. The activation energy (13.19 kcal/mol) calculated for water solution ($\epsilon = 80$), however, is somewhat smaller than the value calculated by Monte Carlo simulation for water solution, 26.3 kcal/mol,[8] or the experimental value, 26.6 kcal/mol.[29] This discrepancy is due to the overestimation of stabilization by sol-

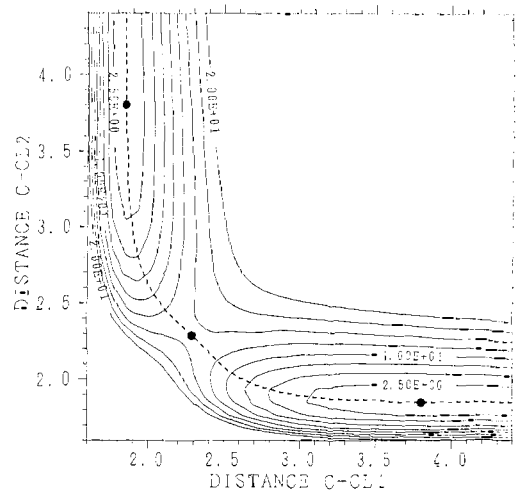

Figure 5. Potential energy map of the $CH_3Cl + Cl^-$ reaction for $\epsilon = 5.0$. See caption of Figure 3.

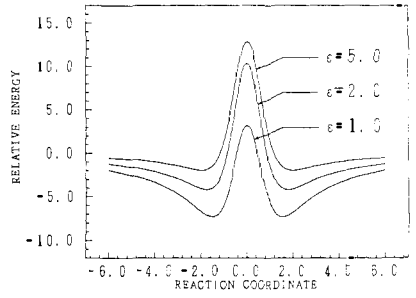

Figure 6. Potential energy curves along the $CH_3Cl + Cl^-$ reaction. The energies are plotted along the dashed line in Figure 3, 4, or 5 as a function of the reaction coordinate, r_c, defined in eq 4. The minimum points correspond to the association complex and the maximum point to the transition state. The energies (in kcal/mol) are relative to that of the separated reactants for each ϵ value.

Table II. Energy Differences (kcal/mol) among the S_R, C_R, and T States of Reaction A

ϵ	$E(C_R) - E(S_R)$	$E(T) - E(S_R)$	$E(T) - E(C_R)$
1	−7.30	3.18	10.48
2	−4.10	10.33	14.43
5	−1.96	12.83	14.79
80	−0.02	13.19	13.39
exptl	−8.6[a]	3.0[b]	11.6[c]
6-31G*[d]	−10.3	3.6	13.9

[a] Gas-phase association enthalpy from ref 28. [b] The value calculated by 11.6 − 8.6. [c] From ref 8. [d] Calculation without solvent. From ref 8.

Table III. Stabilization by Solvation (kcal/mol) at the S_R, C_R, and T States of Reaction A

ϵ	Cl^-	CH_3Cl	S_R	C_R	T
2	−46.1	−1.8	−48.0	−44.8	−40.8
5	−73.8	−3.7	−77.5	−72.1	−67.9
80	−91.1	−5.5	−96.6	−89.5	−86.6
exptl[a]	−81	−5.6	−87		
Monte Carlo[b]			−73		−51

[a] Experimental enthalpies of hydration from ref 30 and 31. [b] From ref 8. The values are enthalpy of hydration estimated by Monte Carlo simulation on an aqueous solution of reactants and the transition state.

(28) Dougherty, R. C.; Roverts, J. D. *Org. Mass Spectrom.* **1974**, *8*, 77.

(29) McLennan, D. J. *Aust. J. Chem.* **1978**, *31*, 1897.

Table IV. Bond Lengths (Å) and Bond Angles (Deg) of the S_R, C_R, T, C_P, and S_P States of Reaction B

state	bond lengths and angles	ϵ = 1.0	ϵ = 2.0	ϵ = 5.0	ϵ = 80
S_R	C-Cl	1.795	1.813	1.834	1.847
	C-H	1.102	1.101	1.100	1.098
	Cl-C-H	108.1	107.2	106.2	105.7
C_R	C-Cl	1.837	1.839	1.847	1.858
	C-F	3.062	3.329	3.591	3.675
	C-H	1.099	1.099	1.098	1.097
	Cl-C-H	106.2	106.1	105.8	105.2
T	C-Cl	1.967	2.067	2.180	2.379
	C-F	2.167	2.057	2.061	2.131
	C-H	1.095	1.093	1.090	1.087
	Cl-C-H	98.3	94.6	92.3	90.2
C_p	C-Cl	3.633	3.851	4.085	4.117
	C-F	1.358	1.360	1.362	1.364
	C-H	1.116	1.115	1.115	1.115
	F-C-H	110.1	110.0	109.8	109.8
S_p	C-F	1.347	1.354	1.360	1.364
	C-H	1.117	1.117	1.116	1.115
	F-C-H	110.6	110.2	109.9	109.7

vation for the transition state species. The stabilization by solvation, ΔE, can be defined by

$$\Delta E = E_{sol} - E_{gas}$$

where E_{sol} and E_{gas} are the energies in solution and in the gas phase, respectively. Table III shows the ΔE value at each stage in the reaction. It shows that the stabilization of the transition state at ϵ = 80 is overestimated. Although the origin of this oversolvation cannot be resolved, the approximate formula, eq 1 and 3, may not sufficiently be correct to describe the solvent effect quantitatively. However, as may be seen from Table III, the relative values of the calculated solvation energy are consistent with the experimental values and with the values calculated by Monte Carlo simulation, and the differential solvation, which is the difference in stabilization by solvation for each molecular state on the reaction coordinate, is correctly evaluated. The present results are thus expected to reproduce well the qualitative feature of the ϵ-dependence of the reaction profile. In the solution with large ϵ, the potential energy well becomes shallow and the energy barrier becomes large (Figure 6). Consequently, the potential energy curve changes shape from the double-well type to the unimodal type when ϵ increases.

The variations of the charge distributions along the reaction coordinate are shown in Figure 7. The charges on the C and Cl atoms increase appreciably with an increase of ϵ, while that of the H atom is not largely affected by ϵ. The positive charge on the C atom becomes greatest at the transition state, r_c = 0.0, irrespective of the dielectric constant. The curve of the Cl atom suggests that the electron transfer from the anion to CH_3Cl occurs around the transition state, and the stabilization that causes the formation of the association complex is due to the electrostatic interaction. The charge distribution is reflected in the differential solvation along the reaction coordinate. This point will be described in detail at the last section.

Reaction of Methyl Chloride with Fluoride Ion. In reaction B, the leaving group is different from the nucleophile and there is energy gap between the reactant and product. The optimized structures for the S_R, C_R, T, C_p, and S_p states are listed in Table IV. The bond lengths C-Cl and C-F increase with an increase of ϵ, except for the C-F bond length at the transition state. The change in the C-H bond lengths was small. A large change of the Cl-C-H angle was observed at the transition state.

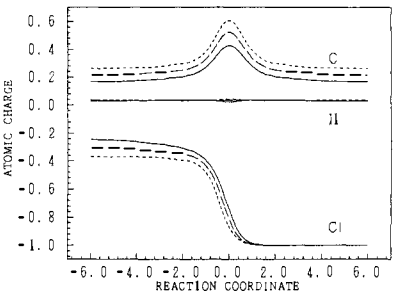

Figure 7. Variations in atomic charges along the reaction coordinate of the $CH_3Cl + Cl^-$ reaction. The solid lines are for ϵ = 1.0, the long dashed lines for ϵ = 2.0, and the short dashed lines for ϵ = 5.0.

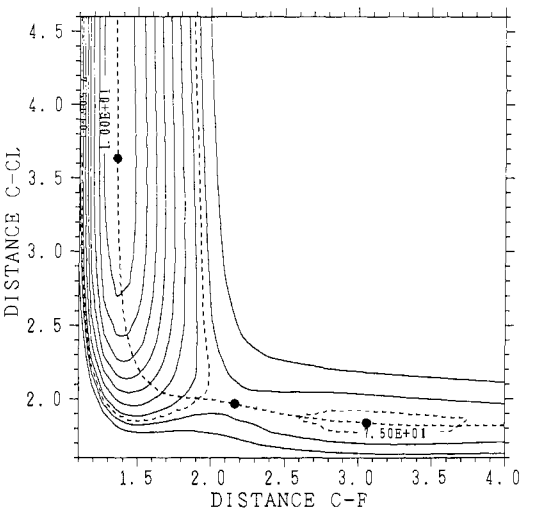

Figure 8. Potential energy map of the $CH_3Cl + F^-$ reaction for ϵ = 1.0. The contours are drawn in steps of 10 kcal/mol. The values are relative to that for the association complex on the product side. The dashed line indicates the reaction path along the reaction coordinate, r_c. The dots indicate the association complexes and the transition state. The C-Cl and C-F distances are in angstroms.

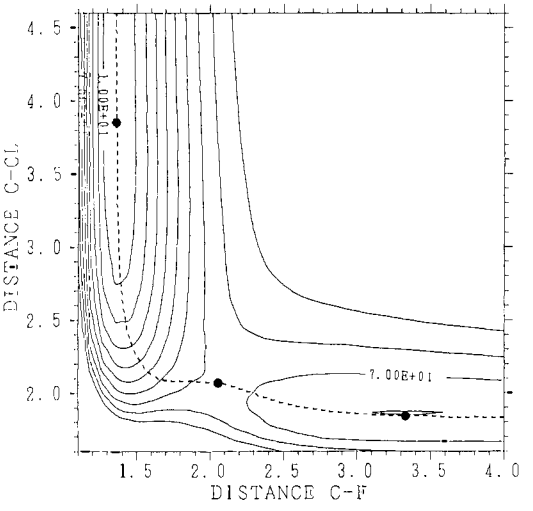

Figure 9. Potential energy map of the $CH_3Cl + F^-$ reaction for ϵ = 2.0. See caption of Figure 8.

Two-dimensional potential energy surfaces of reaction B are shown in Figure 8–10. The ϵ-dependence of the energy surface

Table V. Energy Differences (kcal/mol) among the S_R, C_R, T, C_P, and S_P States of Reaction B

ϵ	$E(S_P) - E(S_R)$	$E(C_R) - E(S_R)$	$E(T) - E(S_R)$	$E(T) - E(C_R)$	$E(C_P) - E(S_P)$	$E(T) - E(S_P)$	$E(T) - E(C_P)$
1	-76.1	-8.5	-3.4	5.1	-5.1	72.7	72.7
2	-60.9	-4.6	8.7	13.3	-2.8	69.6	72.4
5	-51.4	-2.0	14.9	16.9	-1.3	66.3	67.6
80	-45.1	0.0	17.5	17.5	-0.3	62.6	62.9

Table VI. Stabilization by Solvation (kcal/mol) at the S_R, C_R, T, C_P, and S_P States of Reaction B

ϵ	F^-	CH_3Cl	S_R	C_R	T	C_P	S_P	FCH_3	Cl^-
2	-61.5	-1.8	-63.3	-54.5	-51.3	-45.9	-48.1	-2.0	-46.1
5	-98.4	-3.7	-102.1	-95.6	-83.8	-73.7	-77.4	-3.6	-73.8
80	-121.5	-5.5	-126.9	-118.5	-106.0	-91.2	-95.9	-4.9	-91.1

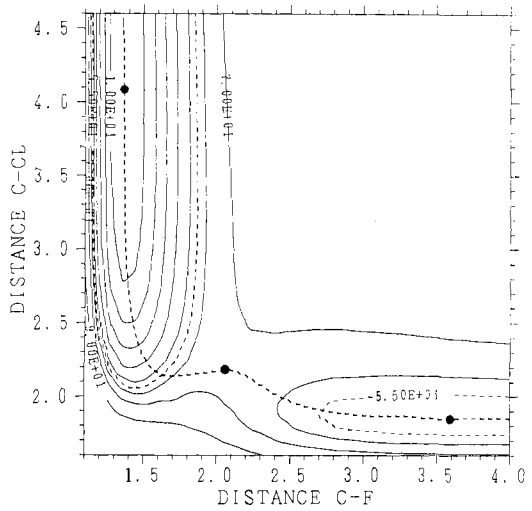

Figure 10. Potential energy map of the $CH_3Cl + F^-$ reaction for $\epsilon = 5.0$. See caption of Figure 8.

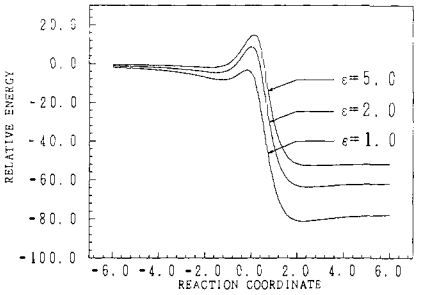

Figure 11. Potential energy curves along the reaction coordinate of the $CH_3Cl + F^-$ reaction. The energies are relative to that of the separated reactants in kcal/mol.

is similar to that observed in reaction A; when ϵ increases, the energy surface becomes flat, although the activation energy increases.

The potential energy profile along the MERP is shown in Figure 11. The energy differences between states are listed in Table V, and the stabilization energy of each molecular state by solvation is shown in Table VI. The heat of reaction calculated by the MNDO method ($\epsilon = 1$), -76.1 kcal/mol, is too large in comparison with the experimental value in the gas phase, -28.5 kcal/mol.[2] This large discrepancy comes from the poor MNDO energy of F^- for $\epsilon = 1$. The MNDO heat of formation of F^- is too positive, although those of Cl^-, CH_3Cl, and CH_3F are reproduced satisfactorily.[7g,23b] The potential energy curve for $\epsilon = 1$ is thus disturbed, and the calculated apparent energy barrier, -3.4 kcal/mol, is smaller than the experimental value in the gas phase, 0.15 kcal/mol.[3] As may be seen from Table VI, the calculated solvation energies of Cl^- (-91 kcal/mol) and F^- (-122 kcal/mol) for $\epsilon = 80$ agree well with the experimental hydration enthalpies, -81 kcal/mol for Cl^- and -113 kcal/mol for F^-.[30,32] It is thus expected that the present method reproduces well the qualitative feature of the ϵ-dependence of the potential energy profile of reaction B. The calculated energy barrier increases with an increase of ϵ. This trend agrees with experiment, although the magnitude of the barrier for $\epsilon = 80$, 17.5 kcal/mol, is smaller than the activation

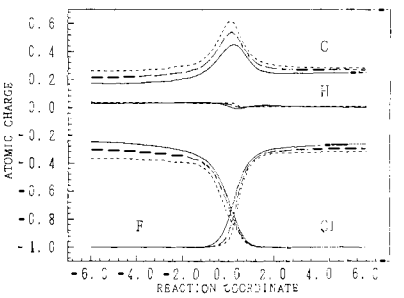

Figure 12. Variations in atomic charges along the reaction coordinate of the $CH_3Cl + F^-$ reaction. The solid lines are for $\epsilon = 1.0$, the long dashed lines for $\epsilon = 2.0$, and the short dashed lines for $\epsilon = 5.0$.

energy in water, 26.9 kcal/mol,[33] as is observed in reaction A.

Reaction B in the gas phase ($\epsilon = 1.0$) reaches the transition state earlier than reaction A; $r_c = -0.20$ and $\angle Cl\text{-}C\text{-}H = 98.3°$. As may be seen from Figure 11, the transition state moves slightly to the reaction product side when ϵ increases; $r_c = 0.00$ for $\epsilon = 2.0$ and $r_c = 0.12$ for $\epsilon = 5.0$. The heat of reaction decreases as ϵ increases. These two trends observed in the potential energy profile support the postulate given by Hammond.[32] The stabilization of the association complex and of the separated state on the product side is less than on the reactant side. This differential solvation is mainly due to the large differences in the stabilization by solvation between Cl^- and F^-. The shift from the double-well potential to the unimodal one is expected for reaction B if the dielectric constant of the solvent increases.

The variations of the charges on the C, Cl, F, and H atoms along the reaction coordinates are shown in Figure 12. The ϵ-dependence of the charges is similar to that observed in reaction A.

Role of Solvation Energy Terms. The concept that the more a solute molecule is polarized, the more the molecule is stabilized by solvation can be understood from the one-center term in eq 1. This term is negative and makes the molecular system stable. The magnitude of stabilization by solvation is determined by this term.

The two-center term in eq 1 is very sensitive to the molecular geometry of the system, and the differential solvation mostly originates from this term in reaction A. When the sum of the electrostatic interactions between atoms in the system is negative, the two-center solvation term becomes positive and works to increase the energy of the system. When an anion approaches a dipolar molecule, the electrostatic attraction between them increases, while the electrostatic repulsion due to the two-center term of solvation energy also increases. The contribution of the repulsive term increases as ϵ increases, and the attraction and repulsion terms between the ion and the dipolar molecule are canceled when $\epsilon \to \infty$. Thus the energy at the association complex becomes equal to that of the separated reactants, as shown in Figure 1 and 2.

The differential solvation in reaction A can be understood qualitatively from the charge distribution of molecular states. Since the atomic charge populations are essentially the same at the S_R and C_R states, the contribution of the one-center term of solvation is same for these two states. At the transition state, the polarization of the C-Cl bond becomes largest (see Figure 7) and the one-center term becomes largest. Thus the order of the stabilization by solvation due to the one-center term is $S_R \simeq C_R < T$. A similar analysis gives that the order of destabilization by solvation due to the two-center term is $S_R < C_R \ll T$. The total

(30) (a) Alexander, D. M.; Hill, D. J. T.; White, L. R. *Aust. J. Chem.* **1971**, *24*, 1143. (b) Ohtaki, H. *Solution Chemistry*; Dainippon Tosho: Tokyo, 1987; p 64.
(31) Rosseinsky, D. R. *Chem. Rev.* **1965**, *65*, 467.
(32) Hammond, G. S. *J. Am. Chem. Soc.* **1955**, *77*, 334.
(33) Bathgate, R. H.; Moelwyn-Hughes, E. A. *J. Chem. Soc.* **1956**, 2642.

stabilization by solvent becomes $S_R > C_R > T$ as shown in Table III. The relative values of the one-center and two-center terms in eq 1 are important in describing the differential solvation correctly. Our results show that eq 3 keeps a good balance between these two terms and therefore gives the correct qualitative picture of solvation energy.

Conclusion

Typical S_N2 reactions of methyl chloride with anions, Cl^- and F^-, were studied on the basis of the MNDO–effective charge model calculation. The potential energy diagram obtained for the reaction in the gas phase ($\epsilon = 1.0$) was the double-well type potential, which has been accepted for the gas-phase reaction profile. For the reaction in solution ($\epsilon > 1.0$), the potential well becomes shallow and the energy barrier becomes higher than that in the gas phase. The shift from a double-well potential to a unimodal type one was shown to occur when the dielectric constant of the solvent is increased. These results support the reaction profile proposed by Brauman et al.[2] and agree well with Monte Carlo simulation by Chandrasekhar et al.[8]

It has been shown that the MNDO–effective charge model represents the differential solvation correctly. Although the effective charge model does not involve the specific interactions between a solute molecule and solvent, the electrostatic interactions between them are fully included. It is thus expected that the method can be applied successfully to qualitatively understand solvation effects due to electrostatic interactions.

Acknowledgment. This work was supported by The University of Tsukuba Research Project.

Registry No. Cl, 16887-00-6; F, 16984-48-8; CH_3Cl, 74-87-3.

Ab Initio Studies of Molecular Structures and Energetics. 2. Energies and Stabilities of PH_n, SH_n, and ClH_n Compounds

Carl S. Ewig* and John R. Van Wazer

Contribution from the Department of Chemistry, Vanderbilt University, Nashville, Tennessee 37235. *Received April 11, 1988*

Abstract: The energies and molecular structures of the highly coordinated species PH_5, SH_4, SH_6, ClH_3, and ClH_5 have been derived by ab initio computations. All structure optimizations employed the MP2 approximation, and energies were computed at the SCF, MP2, and MP4 levels and in two quite different basis sets, in each case with polarization functions on H and the heavy atom. Of particular interest are ClH_3, which is of C_{2v} symmetry, and ClH_5, which is C_{4v}. MP2 vibrational frequencies were determined for each species. Each was found to be structurally stable (i.e., exhibiting no imaginary vibrational frequencies), although a similar treatment of ClH_7 found it to be unstable. The values of $\Delta H°_{298}$ and $\Delta G°_{298}$ were computed for each of the hydrogenation reactions $PH_3 + H_2 \rightarrow PH_5$, $SH_2 + H_2 \rightarrow SH_4$, $SH_4 + H_2 \rightarrow SH_6$, $ClH + H_2 \rightarrow ClH_3$, and $ClH_3 + H_2 \rightarrow ClH_5$ and the analogous reactions for adding two H atoms. In all cases the products are of higher energy than reactants except for the addition of atomic hydrogen to PH_3, SH_2, and SH_4. The energy difference is largest for addition of H_2 to the Cl compounds, $\Delta H°_{298}$ being 477 and 503 kJ/mol for formation of ClH_3 and ClH_5, respectively, at the MP4 level. The energy of each species was analyzed by use of the ab initio multicenter energy resolution, a method of analysis that was found to be an especially powerful way of elucidating the nature of its bonding and hence the origins and degree of its structural stabilities. This analysis demonstrates that three-center bonding stabilizes the Cl species more than the others, while increasing three-center repulsions between neighboring H atoms destabilize all the higher coordinations and lead to the instability of ClH_7.

One of the most important advances to take place in quantum chemistry in recent years has been the development of efficient procedures for ab initio computation of derivatives of molecular energies with respect to bond distances and angles. Such procedures permit the optimization of relatively complex molecular structures and also estimation of all their concomitant vibrational frequencies.

The ability to compute vibrational frequencies is of particular importance in dealing with species which have not been observed in the laboratory since the absence of any imaginary frequencies (assuming the energy gradients have been made to vanish) is a rigorous proof that, at the level of approximation employed, the structure corresponds to a local minimum in the energy. Therefore unless the associated zero-point energy level lies above the top of the potential well the species exhibiting this structure is stable (at low temperatures) with respect to spontaneous deformations to all others.

The term "stability" is often misapplied and misunderstood. In discussing the existence of novel chemical species, it is useful to distinguish clearly between three distinct types: (a) structural stability, corresponding to a species with no imaginary vibrational frequencies; (b) kinetic or chemical stability, implying that in addition to the above the species is not readily altered by its chemical or physical environment; and (c) thermodynamic stability, meaning that in addition to property (a) the thermodynamic equilibria between the species and its possible rearrangements or other reaction products permit detectable amounts of it to exist. Of these, (b), kinetic stability, is by far the most difficult to compute. Also (c), thermodynamic stability, is of special concern for compounds of heavier elements such as those studied here. Therefore we will focus primarily on (a) and (c), the structural and thermodynamic stabilities of the species in question.

An important class of compounds that has drawn increasing interest, both experimentally and theoretically, are those in which the sum of the substituents plus the unshared electron pairs on a given central atom is greater than four—structures often termed "hypervalent" species. Although once thought to be structurally unstable in general due to the inherent nature of their bonding, recent theoretical and experimental data have indicated that many such species are in fact structurally quite stable,[1] with the difficulty in their preparation in the laboratory stemming largely from thermodynamic instabilities.

In this paper we describe ab initio calculations bearing on the structures, energies, and the thermodynamic and structural stabilities of the key sets of neutral compounds PH_n, SH_n, and ClH_n where n is 1, 3, or 5 for Cl; 2, 4, or 6 for S; and 3 or 5 for P. Except for PH (which has a triplet ground state) and ClH_7 (which we have found to be unstable) this series of compounds represents

0002-7863/89/1511-1552$01.50/0